THE UNIVERSITY of EDINBURGH

Edinburgh Research Explorer

# Increased levels of UCHL1 are a compensatory response to disrupted ubiquitin homeostasis in spinal muscular atrophy and do not represent a viable therapeutic target

**Citation for published version:**
Powis, RA, Mutsaers, CA, Wishart, TM, Hunter, G, Wirth, B & Gillingwater, TH 2014, 'Increased levels of UCHL1 are a compensatory response to disrupted ubiquitin homeostasis in spinal muscular atrophy and do not represent a viable therapeutic target', *Neuropathology and Applied Neurobiology*, vol. 40, no. 7, pp. 873-887. https://doi.org/10.1111/nan.12168

**Digital Object Identifier (DOI):**
10.1111/nan.12168

**Link:**
Link to publication record in Edinburgh Research Explorer

**Document Version:**
Peer reviewed version

**Published In:**
Neuropathology and Applied Neurobiology

**Publisher Rights Statement:**
This article has been accepted for publication and undergone full peer review but has not been through the copyediting, typesetting, pagination and proofreading process, which may lead to differences between this version and the Version of Record. Please cite this article as doi: 10.1111/nan.12168

**General rights**
Copyright for the publications made accessible via the Edinburgh Research Explorer is retained by the author(s) and / or other copyright owners and it is a condition of accessing these publications that users recognise and abide by the legal requirements associated with these rights.

**Take down policy**
The University of Edinburgh has made every reasonable effort to ensure that Edinburgh Research Explorer content complies with UK legislation. If you believe that the public display of this file breaches copyright please contact openaccess@ed.ac.uk providing details, and we will remove access to the work immediately and investigate your claim.

Download date: 06. May. 2023

Accepted Article

# Increased levels of UCHL1 are a compensatory response to disrupted ubiquitin homeostasis in spinal muscular atrophy and do not represent a viable therapeutic target

Rachael A. Powis[1,2], Chantal A. Mutsaers[1,2], Thomas. M. Wishart[1,3], Gillian Hunter[1,2], Brunhilde Wirth[4] & Thomas H. Gillingwater[1,2]*

[1]Euan MacDonald Centre for Motor Neurone Disease Research, [2]Centre for Integrative Physiology, University of Edinburgh, UK
[3]Division of Neurobiology, The Roslin Institute and Royal (Dick) School of Veterinary Studies, University of Edinburgh, UK
[4]Institute of Human Genetics, Institute for Genetics and Center for Molecular Medicine Cologne, University of Cologne, Germany

* Corresponding Author:

Professor Thomas Gillingwater
Euan MacDonald Centre for Motor Neurone Disease Research & Centre for Integrative Physiology
University of Edinburgh
Edinburgh
EH8 9XD
UK
Email: T.Gillingwater@ed.ac.uk
Tel: +44 (0)131 6503724

**Keywords**: Spinal Muscular Atrophy, SMA, UCHL1, Uba1, Ubiquitin

**Running title**: UCHL1 in SMA

This article has been accepted for publication and undergone full peer review but has not been through the copyediting, typesetting, pagination and proofreading process, which may lead to differences between this version and the Version of Record. Please cite this article as doi: 10.1111/nan.12168

This article is protected by copyright. All rights reserved.

**ABSTRACT**

**Aim:** Levels of ubiquitin carboxyl-terminal hydrolase L1 (UCHL1) are robustly increased in spinal muscular atrophy (SMA) patient fibroblasts and mouse models. We therefore wanted to establish whether changes in UCHL1 contribute directly to disease pathogenesis, and to assess whether pharmacological inhibition of UCHL1 represents a viable therapeutic option for SMA.

**Methods:** SMA mice and control littermates received a pharmacological UCHL1 inhibitor (LDN-57444) or DMSO vehicle. Survival and weight were monitored daily, a righting test of motor performance was performed, and motor neuron loss, muscle fibre atrophy and neuromuscular junction pathology were all quantified. Ubiquitin-like modifier activating enzyme 1 (Uba1) was then pharmacologically inhibited in neurons *in vitro* to examine the relationship between Uba1 levels and UCHL1 in SMA.

**Results:** Pharmacological inhibition of UCHL1 failed to improve survival, motor symptoms, or neuromuscular pathology in SMA mice and actually precipitated the onset of weight loss. LDN-57444 treatment significantly decreased spinal cord mono-ubiquitin levels, further exacerbating ubiquitination defects in SMA mice. Pharmacological inhibition of Uba1, levels of which are robustly reduced in SMA, was sufficient to induce accumulation of UCHL1 in primary neuronal cultures.

**Conclusion:** Pharmacological inhibition of UCHL1 exacerbates rather than ameliorates disease symptoms in a mouse model of SMA. Thus, pharmacological inhibition of UCHL1 is not a viable therapeutic target for SMA. Moreover, increased levels of UCHL1 in SMA likely represent a downstream consequence of decreased Uba1 levels, indicative of an attempted supportive compensatory response to defects in ubiquitin homeostasis caused by low levels of SMN protein.

**List of abbreviations for reference:**

SMA: Spinal Muscular Atrophy

SMN: Survival Motor Neuron

UCHL1: Ubiquitin carboxyl-terminal hydrolase L1

Uba1: Ubiquitin-like modifier-activating enzyme 1

UPS: ubiquitin proteasome system

DUB: deubiquitinating enzyme

Accepted Article

This article is protected by copyright. All rights reserved.

## INTRODUCTION

Spinal muscular atrophy (SMA) is a neuromuscular disorder that, with an incidence of ~1 in 6,000 to 1 in 10,000 live births, is a leading genetic cause of infant death (1, 2). SMA is an autosomal recessive disease caused by homozygous disruption of the *survival motor neuron 1* gene (*SMN1*) (3), which results in the hallmark symptoms of lower motor neuron degeneration, muscle atrophy and progressive paralysis (2). The survival motor neuron (SMN) protein is ubiquitously expressed and has well characterised functions in spliceosomal small nuclear ribonucleoprotein assembly and pre-mRNA splicing (4). A second almost identical gene, *survival motor neuron 2* (*SMN2*) is present in humans (3), however, due to a single base pair difference in exon 7, the majority of *SMN2* mRNA transcripts are alternatively spliced and produce a rapidly degraded truncated version of the SMN protein called SMNΔ7 (5, 6). Therefore, only a small proportion of the full-length functional SMN protein as generated by *SMN2* is ultimately translated in SMA patients (2). SMA disease severity is dependent on the amount of functional SMN protein and therefore inversely correlated to *SMN2* copy number (7-9). Clinically, SMA can be classified in to four main types, based principally on the age of onset and ability to reach motor milestones. The most severe form (Type I; with patients possessing one or two *SMN2* copies) affects infants under six months with death usually occurring in the first two years of life (10). Recent advances in translational research have identified potential SMN-dependent and SMN-independent modifiers and therapies for SMA (11-14). However, at present no effective treatments are available (15).

Dysregulation of the ubiquitin proteasome system (UPS) is involved in the pathogenesis of many neurodegenerative diseases (16) and targeting specific components of the UPS may provide a promising strategy for a variety of neurodegenerative disorders, including SMA (17, 18). Many proteins, including SMN (19), are regulated by the UPS, where targeting to the proteasome occurs by way of linkage of poly-ubiquitin chains to the target protein, mediated by three ubiquitinating enzymes known as E1 (ubiquitin-activating), E2 (ubiquitin-conjugating) and E3 (ubiquitin ligase) (20, 21). Protein ubiquitination is a reversible process and is highly regulated by a specific class of proteases, known as deubiquitinating enzymes (DUBs), which cleave ubiquitin from protein substrates (12, 22). Pharmacological inhibition of the proteasome has been shown to increase SMN levels *in vitro* and *in vivo* (23). Moreover, abnormal granular ubiquitin deposits have also been reported in ballooned lower motor neuron cell bodies and higher brain structures of SMA patients (24, 25).

We recently demonstrated widespread disruption of ubiquitin homeostasis in mouse models of SMA (26), including significantly reduced levels of the ubiquitin-like modifier activating enzyme 1 (Uba1) and increased levels of ubiquitin carboxyl-terminal hydrolase L1 (UCHL1) (26). UCHL1 has previously been shown to regulate SMN protein levels in cell culture experiments, where over-expression of UCHL1 reduced SMN levels and conversely pharmacological inhibition or UCHL1 specific knockdown significantly increased SMN expression (27). Importantly, elevated levels of UCHL1 have also been reported in fibroblasts from SMA patients (27). UCHL1 is a highly-conserved DUB that is strongly expressed in

This article is protected by copyright. All rights reserved.

Accepted Article

neuronal cells (28). It is one of the most abundant proteins in the brain, making up 1-2% of the total soluble fraction (29). UCHL1 acts as a deconjugating enzyme releasing monomeric ubiquitin through its C-terminal hydrolytic activity (30), however, it also has reported ligase activity (31) and can also act as a monoubiquitin stabiliser (32). UCHL1 has been implicated in the pathology of several other neurodegenerative disorders including Alzheimer's disease (33, 34), Parkinson's disease (35-39), and an early onset progressive neurodegenerative syndrome (40).

Taken together, the previous studies showing increased levels of UCHL1 in SMA animal models and patient cells suggest that UCHL1 may be contributing to disease pathogenesis and that inhibition of UCHL1 may therefore offer an attractive therapeutic approach for the treatment of SMA. The aim of this study was to investigate the role of UCHL1 in disease pathogenesis and to establish whether pharmacological inhibition of UCHL1 would improve survival and motor symptoms in an established mouse model of severe SMA. We show that pharmacological inhibition of UCHL1 in SMA mice had no effect on SMN levels *in vivo* and did not improve survival or motor symptoms, but rather precipitated the onset of weight loss. We also demonstrate that increased levels of UCHL1 observed in SMA are actually, at least in part, a downstream consequence of decreased levels of Uba1, suggestive of an attempted compensatory response to defects in ubiquitin homeostasis caused by low levels of SMN.

Accepted Article

This article is protected by copyright. All rights reserved.

## MATERIALS AND METHODS

### Ethics statement

Experimental procedures conducted in this study were performed in accordance with the UK Animals (Scientific Procedures) Act 1986. All animal experiments were approved by a University of Edinburgh internal ethics committee and were performed under Home Office project license numbers 60/3891 and 60/4569. For primary cell culture of human fibroblasts, informed consent was previously obtained from all patients and their parents.

### SMA patient and control fibroblast cell culture

Human fibroblasts were previously obtained from skin biopsies from three SMA Type I patients: ML 16, ML 17, ML 83 and three age matched unaffected controls: ML 24, ML 32, ML 44. Molecular analysis confirmed that all SMA patients had homozygous deletion of *SMN1*. Cells were maintained in high glucose Dulbecco's modified Eagle medium (DMEM) (Gibco, Invitrogen) supplemented with 10% heat inactivated foetal bovine serum (HyClone, Thermo Scientific) and 100U/ml penicillin and 100mg/ml streptomycin (Gibco, Invitrogen). Fibroblasts were expanded and harvested for protein on or below passage eight.

### SMA mouse model

The 'Taiwanese' model of severe SMA (*Smn*$^{-/-}$; *SMN2*$^{tg/0}$) (41, 42) was used for the *in vivo* characterisation of pharmacological UCHL1 inhibition in these experiments. Taiwanese mice represent a good model for pre-clinical SMA drug testing as their increased lifespan (compared to other severe SMA mouse models) enables a longer drug dosing regime and motor function tests to be performed (26, 42, 43). Taiwanese SMA mice on a congenic FVB background were originally obtained from Jackson Laboratories and maintained under standard SPF conditions at the University of Edinburgh. Phenotypically normal heterozygous *Smn*$^{+/-}$; *SMN2*$^{tg/0}$ littermates were used as controls.

### UCHL1 immunohistochemistry

Following termination by overdose of anaesthetic, the vertebral columns and *gastrocnemius* muscles were rapidly dissected from P10 SMA and control mice and fixed overnight in 4% paraformaldehyde in phosphate buffered saline (PBS), before being transferred to a 30% sucrose solution overnight at 4 °C for cryoprotection. Tissue was embedded in optimal cutting temperature compound (OCT) and stored at -80 °C before being sectioned at 20 µm using a cryostat and collected directly on to slides. Sections were blocked in IgG and protease-free standard blocking solution (0.2% bovine serum albumin [BSA], 0.5% Triton X-100 in PBS) for 30 min at room temperature before overnight incubation with rabbit anti-mouse UCHL1 primary antibody (1:500 diluted in blocking solution, Novus Biologicals, Cambridge, UK, NB300-676) at 4 °C. After 6 x 5min washes in PBS, sections were incubated with swine anti-rabbit IgG TRITC secondary antibody (1:100 diluted in PBS, DAKO, Denmark, R0156) for 1h at 4 °C and then mounted and cover slipped in a 10% Mowoil solution (Polyscience). Secondary only control sections were treated in an identical manner except for the exclusion of primary antibody (Supplementary Figure S1). Sections were viewed using an inverted Olympus 1X71 microscope with either a 10x or 20x objective

This article is protected by copyright. All rights reserved.

Accepted Article

and images taken using a digital CCD camera (Hamamatsu C4742-95) and OpenLab (Improvision) image capture software.

**UCHL1 inhibitor administration**

LDN-57444 (Calbiochem) is an isatin O-acyl oxime compound that acts as a potent, reversible, competitive, and active site-directed inhibitor of UCHL1 ($K_i$ = 0.40 µM; $IC_{50}$ = 0.88 µM) with ~28-fold greater selectivity over UCHL3. LDN-57444 was dissolved in dimethyl sulfoxide (DMSO) and administered 0.5 mg/kg, twice daily to SMA and control mice via intraperitoneal (i.p) injection from the day of birth (P1). This dose was based on previous studies reporting this concentration to be effective *in vivo* (34, 44). The same volume of DMSO was administered by i.p injection to SMA and littermates as a vehicle-only control. Litters were randomly assigned to either LDN-57444 or vehicle only treatment groups. Survival and weight were monitored on a twice-daily basis. The age of weight loss onset was defined as the first day at which an individual animal showed a reduction in body weight. Mice were retroactively genotyped using standard PCR methods (42, 45).

**Motor performance test**

To assess the impact of UCHL1 inhibition on motor performance a righting reflex test was performed on mice at P3, P6 and P9. The righting reflex is a commonly used (26, 46), simple assay to assess motor ability in neonatal mice and was performed by placing a mouse on its back on a flat surface and measuring the time taken to turn over onto its paws (46). If a mouse did not respond within 60 seconds the test was terminated.

**Primary hippocampal neuronal culture**

E17 rat hippocampal neurons were cultured in Basal Medium Eagle (BME) serum free medium complemented with 1.6% of a 32.5% glucose solution, 1% Sodium Pyruvate 100 nM solution, 1% N-2 supplement and 5% B27 supplement. Cells were plated in a12-well plate and kept in 1ml of media. The cells were treated with 50uM UBEI-41, a cell-permeable ubiquitin E1 inhibitor (26) with an IC50 ~ 5 µM (Biogenova) dissolved in DMSO or DMSO only vehicle control for 2 hours before the cells were harvested by lysing the cells using Radio-Immunoprecipitation Assay (RIPA) buffer.

**Protein extraction and concentration determination**

To determine UCHL1 protein levels in SMA mice and control littermates, whole spinal cord tissue and *gastrocnemius* muscle was quickly dissected and frozen on dry ice. To establish if the LDN-57444 dosing regieme was effective at altering ubiquitin or SMN levels *in vivo*, whole spinal cord tissue was dissected from P10 mice which had been treated twice daily with LDN-57444 or vehicle. All protein extracted from tissue and cell lysate was homogonised and extracted in RIPA buffer (ThermoScientific) with protease inhibitor cocktail (Sigma) and the protein concentration determined by BCA assay (ThermoScientific).

**Quantitative fluorescent western blot analysis**

Extracted protein was separated by SDS–polyacrylamide gel electrophoresis on 4–20% precast NuPage 4–12% BisTris gradient gels (Invitrogen) and then transferred to PVDF

This article is protected by copyright. All rights reserved.

Accepted Article

membrane by the iBlot 7 minute semi-dry blotting system (Invitrogen). Total protein levels were determined by incubation of each blot in a solution of Ponceau S (0.2% Ponceau, 30% acetic acid). PVDF membranes were then placed in blocking solution (Li-Cor) for 30 min at room temperature and quantitative western blots performed using primary antibodies against rabbit anti-mouse UCHL1 (1:2000, Novus Biologicals, NB300-676), mouse anti-ubiquitin (1:1000, clone Uba-1 [aka 042691GS], Merck Millipore, MAB1510), mouse anti-human SMN (1:1000, BD Biosciences) and mouse anti-beta-actin (1:1000, Abcam, Ab8226) all diluted in blocking solution overnight at 4 $^{o}$C. Following 6 x 5min washes in PBS, Odessey secondary antibodies (goat anti-rabbit IRDye 680 or donkey anti-mouse IRDye 680, LI-COR Biosciences) were diluted in blocking buffer according to the manufacturers' instructions and added to membranes for 1 hour at room temperature. Blots were washed for 6 x 5min in PBS, dried and imaged using an Odyssey Infrared Imaging System (Li-COR, Biosciences). Each blot was scanned and fluorescent band intensity measured in triplicate to minimise user variability. Due to alteration in the expression levels of many standard loading control proteins in SMA tissues (47), total protein levels, as measured by Ponceau S, were used as a loading control.

**Motor neuron cell body counts**

Mice were sacrificed at P8 (N=4 per genotype/treatment) and the spinal column was removed before immersion in a 4% paraformaldehyde (in PBS) solution overnight at 4$^{o}$C. The spinal cord was then removed from the column and placed in a 30% sucrose solution overnight for cryoprotection. The lumbar enlargement was then dissected and placed in OCT, frozen on dry ice and stored at -80$^{o}$C. 20µM sections were cut on a cryostat and every fourth section collected onto superfrost slides. For Nissl staining, slides were brought to room temperature, rinsed in water, dehydrated through graded alcohols (70%, 90% and 100% ethanol) before being paced in xylene for 10 minutes. Sections were then rehydrated back down the graded alcohols and water before being stained in 0.2% Cresyl Fast Violet containing 1% acetic acid for 7 minutes. Following dehydration through graded alcohol solutions and xylene, slides were cover-slipped using DPX mounting media. Phase contrast images of the ventral horn were taken using an inverted Olympus 1X71 microscope with a 4x objective and images taken using a digital CCD camera (Hamamatsu C4742-95) and OpenLab (Improvision) image capture software. Counts of motor neuron cell soma were performed by an investigator blind to the genotype and treatment status of each specimen, as previously described (26).

**Neuromuscular junction immunohistochemistry**

Mice were sacrificed at P8 (N=3 per genotype/treatment) and the *levator auris longus* (LAL) and *transversus abdominis* (TVA) muscles were dissected and immunohistochemically labelled as previously described (45). Counts of the number of motor axons innervating each neuromuscular junction were performed by an investigator blind to the genotype and treatment status of each specimen, as previously described (26).

**Muscle fibre diameter measurements**

Mice were sacrificed at P8 (N=3 per genotype/treatment) and whole-mount teased fibre preparations of LAL and TVA muscles were prepared as previously described (26). Phase

This article is protected by copyright. All rights reserved.

Accepted Article

contrast images of isolated single muscle fibres were taken using an inverted Olympus 1X71 microscope at 20x objective equipped with a digital CCD camera (Hamamatsu C4742-95) and OpenLab (Improvision) image capture software. Muscle fibre diameters were measured using ImageJ software by an investigator blind to the genotype and treatment status of each specimen, as previously described (26).

**Statistical analysis**

Data were analysed using Microsoft Excel and GraphPad Prism software. All data are reported as mean ± SEM. Individual statistical tests used are detailed in figure legends. Statistical significance was considered to be $P \leq 0.05$ for all analyses. Figures were created using Adobe Photoshop.

Accepted Article

This article is protected by copyright. All rights reserved.

## RESULTS

### Increased UCHL1 levels in Type I SMA patient fibroblasts

In order to confirm previous reports of elevated UCHL1 levels in SMA patients (27), western blot analysis was performed on protein extracted from Type I SMA primary patient fibroblasts and fibroblasts from unaffected controls. UCHL1 was found to be significantly increased in Type I SMA patient fibroblasts compared to unaffected controls (control 100% ± 48.8% vs. SMA 6000% ± 671.9&, N = 3, $P < 0.01$) (Figure 1A and B), with a similar large magnitude of change to that previously reported by Hsu and colleagues (27).

### UCHL1 levels are increased in SMA mouse spinal cord and muscle

As well as data from SMA patient fibroblasts (27), previous studies have demonstrated increased levels of UCHL1 in isolated synaptic preparations from the 'severe' mouse model of SMA (26). Initially, therefore, we wanted to establish whether UCHL1 levels were similarly increased throughout the neuromuscular system of the 'Taiwanese' mouse model of SMA (42). Western blot analysis of whole spinal cord and *gastrocnemius* muscle protein from 'Taiwanese' SMA mice compared to unaffected littermate controls at P10 revealed that UCHL1 levels were significantly elevated in the spinal cord (control 100% ± 9.1%, N=4 vs. SMA 269.0% ± 18.3%, N=4, $P < 0.005$) (Figure 2A and B) and muscle (control 100% ± 12.1%, N=3 vs. SMA 304.3% ± 41.2%, N=4, $P < 0.01$) (Figure 2D and E). Similarly, increased levels of UCHL1 were present in the ventral horn of spinal cord and *gastrocnemius* muscle from 'Taiwanese' SMA mice compared to littermate controls when visualised using immunohistochemical techniques (Figure 2C and F). A temporal analysis of UCHL1 levels in muscle revealed significantly elevated UCHL1 levels present from early- through to late-symptomatic time points (P4: control 100% ± 13.5%, N=3 vs. SMA 142.8% ± 20.2%, N=3, $P < 0.05$, P7: control 100% ± 33.9%, N=3 vs. SMA 220.5% ± 52.0%, N=3, $P < 0.05$), but not at a pre-symptomatic age (P1: control 100% ± 28.1%, N=3 vs. SMA 95.8% ± 24.6%, N=3) (Figure 2G).

### Pharmacological inhibition of UCHL1 reduced ubiquitin levels in the SMA mouse spinal cord *in vivo* but did not affect SMN levels

In order to determine the effects of inhibiting UCHL1 on SMA pathogenesis *in vivo*, we identified LDN-57444 as a potent pharmacological inhibitor. Treatment with LDN-57444 has been shown to significantly reduce ubiquitin levels in the mouse brain (44), with measurement of mono-ubiquitin levels established as a good marker for UCHL1 *in vivo* activity (48). Whole litters of mice (including both 'Taiwanese' SMA mice and littermate controls) were dosed twice daily with 0.5 mg/kg of LDN-57444 (or vehicle only control) via intraperitoneal (i.p) injection, starting at the day of birth. Litters were randomly assigned to either LDN-57444 or vehicle only treatment groups.

Mono-ubiquitin levels were measured using quantitative western blot analysis on whole spinal cord tissue from animals culled at P10. Pharmacological inhibition of UCHL1 significantly reduced levels of monomeric ubiquitin by ~20% *in vivo* compared to vehicle controls (Figure 3A and B). This is a similar reduction to that previously reported in neurons

This article is protected by copyright. All rights reserved.

Accepted Article

treated with LDN-57444 *in vitro* (48), indicating that the dosing regime was effective at inhibiting UCHL1 hydrolase activity in SMA mice *in vivo*. In contrast to previous SMA fibroblast *in vitro* data (27), pharmacological inhibition of UCHL1 did not increase SMN levels in SMA mice *in vivo* (vehicle 100% ± 22.83% vs. LDN-57444 99.29% ± 28.53%, N=3) (Figure 3C and D).

**Pharmacological inhibition of UCHL1 failed to improve weight or survival of SMA mice, and precipitated the onset of weight loss**

To establish the effect of pharmacological inhibition of UCHL1 on SMA mice, we initially measured the weight of SMA mice daily from birth. Treatment with LDN-57444 did not modify the average daily weight of SMA mice (Figure 4A), nor did it modify the average daily weight of littermate control mice (Figure 4A). However, the age at which weight loss was first observed in SMA mice (an indicator of overt disease onset) was significantly reduced in the LDN-5744 treated animals, suggesting that UCHL1 inhibition actually had a detrimental impact on disease progression ($P < 0.05$) (Figure 4C).

Next, we performed a survival analysis on LDN-57444 and vehicle-only control treated SMA mice. The survival curve of LDN-57444 treated mice was shifted to the left of the vehicle treated curve (Figure 4B), indicating that if anything LDN-57444 was precipitating the onset of disease, although the median survival did not reach statistical significance (median age of death of vehicle treated SMA mice was P11, N=11 vs. P10 for LND-57444 treated SMA mice, N=10) (Figure 4B).

**Pharmacological inhibition of UCHL1 did not improve motor performance of SMA mice**

To further assess the impact of UCHL1 inhibition on neuromuscular phenotypes in SMA mice, we monitored motor performance using the righting reflex test at postnatal day three (P3), six (P6) and nine (P9). At P3 there was no significant difference between the righting times observed in SMA and littermate control mice, with LDN-57444 having no observable effect (Figure 4A). However, at P6 and P9 both SMA vehicle and SMA LDN-57444 treated mice performed significantly worse than control vehicle and control LDN-57444 treated mice (for all comparisons $P < 0.05$) (Figures 5B and C). At all three time points LDN-57444 administration had no significant impact on the motor performance of SMA mice (Figure 5A, B and C). At P6 vehicle treated SMA mice took 9 ± 2 seconds to right (N=15), whereas LDN-57444 treated SMA mice took 8 ± 2 seconds (N=9) (Figure 5B). At P9 the average righting time was 7 ± 3 seconds (N=11) for vehicle treated SMA mice compared to 9 ± 2 seconds for LDN-57444 treated SMA mice (N=6) (Figure 5C). Thus, treatment with LDN-57444 had no measurable effect on motor performance in SMA mice.

**Pharmacological inhibition of UCHL1 did not improve neuromuscular pathology in SMA mice**

To determine whether UCHL1 inhibition was having a sub-clinical impact on underlying neuromuscular pathology in SMA mice, we assessed motor neuron soma loss from the ventral horn of spinal cord, skeletal muscle fibre atrophy and neuromuscular junction

This article is protected by copyright. All rights reserved.

Accepted Article

pathology in LDN-57444 treated SMA mice at a late-symptomatic time-point (P8). As previously reported for the 'Taiwanese' mouse model of SMA (26, 42), there was a modest, but statistically significant, loss of motor neurons from the ventral horn of spinal cord at late-symptomatic time-points compared to littermate controls (Figure 6A and B). Motor neuron loss was not ameliorated in SMA mice treated with LDN-57444 (Figure 6A and B; N=4 mice per genotype/treatment). Similarly, skeletal muscle fibre atrophy has previously been documented in the 'Taiwanese' SMA mice (26). Treatment with LDN-57444 had no significant impact on this process in either the LAL or TVA muscle (Figure 6C, D and E; N=3 mice). Likewise, treatment with LDN-57444 had no impact on the modest loss of axonal inputs observed from neuromuscular junctions in late-symptomatic SMA mice (Figure 6F and G; N=3 mice).

**Uba1 inhibition increased UCHL1 levels *in vitro***

The observation that pharmacological inhibition of UCHL1 exacerbated, rather than improved, the health of SMA mice, alongside the observation that inhibition of UCHL1 led to a decrease in mono-ubiquitin levels *in vivo* (thereby phenocopying ubiquitination defects previously reported in SMA mice; (26)), led us to question whether increased levels of UCHL1 in SMA actually represent an attempted compensatory response, rather than driving neuromuscular pathology. We therefore wanted to establish whether increased levels of UCHL1 were caused by upstream changes in other aspects of the ubiquitin pathway known to be altered in SMA. Given that we previously demonstrated that low levels of SMN lead to reduced levels of the E1 ubiquitin-activating enzyme Uba1 in SMA mice (~50% of those seen in healthy control mouse spinal cord and ~40% of those present in healthy mouse skeletal muscle (26)), and that genetic or pharmacological suppression of Uba1 is sufficient to recapitulate SMA-like neuromuscular pathology in zebrafish (26), we examined whether increased levels of UCHL1 were occurring as a direct response to lowered Uba1 levels.

We treated primary neurons with UBEI-41, a potent pharmacological Uba1 inhibitor (49, 50), for 2 hours and examined the effect on UCHL1 levels. Cells treated with UBEI-41 had significantly reduced mono-ubiquitin levels compared to untreated controls (Figure 7A and B), confirming targeting of Uba1 and downstream Uba1-dependent ubiquitination pathways (26). Strikingly, UCHL1 levels were robustly increased (>3-fold) in cells treated with UBEI-41 (Figure 7A and C). Thus, pharmacological suppression of Uba1 (phenocopying the reduced levels of Uba1 in SMA mouse spinal cord and muscle; (26)) was sufficient to increase UCHL1 levels in neurons. This finding suggests that the increased levels of UCHL1 observed in SMA are, at least in part, a downstream consequence of SMN-mediated Uba1 suppression. Taken together with our findings regarding the negative influence of UCHL1 inhibition on SMA mice, this suggests that increased levels of UCHL1 likely represent an attempted compensatory response to defects occurring elsewhere in the UPS.

This article is protected by copyright. All rights reserved.

Accepted Article

Accepted Article

## DISCUSSION

Previous findings from animal models of SMA and patient fibroblasts suggested that increased levels of UCHL1 may be contributing to disease pathogenesis in SMA, leading to the suggestion that inhibition of UCHL1 might offer an attractive therapeutic approach for the treatment of SMA (26, 27). In the present study, we confirm and extend these initial observations by showing that UCHL1 levels are significantly increased in the neuromuscular system *in vitro* and *in vivo* during SMA. However, in contrast to the initial suggestions that inhibition of UCHL1 might represent a therapeutic target for SMA, pharmacological inhibition of UCHL1 in SMA mice failed to improve survival, motor symptoms or neuromuscular pathology, and instead precipitated the onset of weight loss. This worsening of overt disease status could be explained by the observation that pharmacological inhibition of UCHL1 *in vivo* significantly decreased spinal cord mono-ubiquitin levels, thereby exacerbating ubiquitination defects previously reported in SMA mice (26). This finding, together with the known DUB role of UCHL1, suggests that the increased UCHL1 levels present in SMA actually represent an attempted compensatory response to help increase and restore ubiquitin homeostasis. We demonstrated that pharmacological inhibition of the E1 enzyme Uba1 in primary neuronal cell culture, phenocopying the situation observed in SMA mouse spinal cord and muscle (26), was sufficient to robustly increase UCHL1 expression *in vitro*. This indicates that the increased levels of UCHL1 observed in SMA are, at least in part, a downstream consequence of Uba1 suppression and are likely to represent a response to upstream defects in ubiquitin homeostasis previously shown to be caused by low levels of SMN (26).

Maintenance of ubiquitin homeostasis is crucial to nervous system development and function (51) with DUBs such as UCHL1 playing crucial roles in the conservation of ubiquitin levels and prevention of inappropriate target degradation by the proteasome (52). The importance of UCHL1 activity to the nervous system is underscored by the association of several UCHL1 loss-of-function mutations with neurodegenerative diseases and the neurodegenerative phenotypes reported in experimental models of UCHL1 inhibition. The G7A missense mutation in the *UCHL1* gene reduces ubiquitin binding affinity causing a near complete loss of UCHL1 hydrolytic activity and is linked to a severe early-onset neurodegenerative syndrome (40). Similarly, the I93M *UCHL1* mutation, which confers a 50% reduction in catalytic activity, has been reported in a family with autosomal dominant Parkinson's disease (35) with expression of the I93M mutant in transgenic mice leading to the degeneration of dopaminergic neurons (53). Conversely, the S18Y polymorphism variant of *UCHL1*, which has comparable hydrolase but reduced ligase activity, has been associated with a decreased Parkinson's disease risk (31, 54). Down-regulation of *UCHL1* has been reported in Alzheimer's disease brains where the number of neurofibrillary tangles is inversely proportional to soluble UCHL1 levels (55). In the *APP/Ps1* mouse model of Alzheimer's UCHL1 has been shown to be important in synaptic function and contextual memory (34). *In vitro* application of LDN-57444 to hippocampal slices reduced long-term potentiation whilst transduction of UCHL1 protein corrected defects in synaptic transmission and improved fear learning *in vivo* (34). However, other studies have found potential beneficial effects of

This article is protected by copyright. All rights reserved.

pharmacological inhibition of UCHL1 by LDN-57444 for Parkinson's disease treatment by enhancing clearance and reducing alpha-synuclein levels (44). Interestingly, in non-transgenic animals and neuronal cells with endogenous UCHL1 levels LDN-57444 treatment produced the opposite effect on alpha-synuclein distribution, highlighting the different effects UCHL1 inhibition can have under normal and pathological conditions (44).

UCHL1 knock-out mice present with progressive paralysis and premature death associated with progressive degeneration of pre-synaptic terminals and marked impairment of synaptic transmission at the neuromuscular junction (NMJ) (56). Similarly, ubiquitin deficiency caused by loss of the DUB Usp14 in *ataxia* mice has been shown to cause selective developmental defects at the motor endplate and disruption of synaptic transmission, with transgenic restoration of ubiquitin levels preventing pathology (52). These striking similarities of NMJ vulnerability due to the loss of DUBs could be due the high demand of the UPS in endplate development coupled with the long distances of ubiquitin transport making motor neurons particularly vulnerable to local fluctuations in ubiquitin levels (52). Interestingly, NMJ denervation caused by loss of presynaptic inputs is also observed in early symptomatic SMA mice (45). A spontaneous mutation in the *Uch-L1* gene, which causes loss of detectable UCHL1 protein expression, is present in *gracile axonal dystrophy* (*gad*) mice (57). *Gad* mice display progressive accumulation ubiquitinated protein conjugates alongside axonal degeneration of the gracile tract along with motor paresis (58). Recently, it has also been shown that eGFP expression driven by the *Uch-L1* promoter genetically labels a subpopulation of degeneration resistant spinal motor neurons in a mouse model of amyotrophic lateral sclerosis (59). Together, these findings indicate that the increased UCHL1 levels observed in SMA may in fact represent an attempted compensatory response to defects occurring elsewhere in the UPS (e.g. to Uba1), and may therefore actually represent an attempted neuroprotective response (akin to the situation reported in amyotrophic lateral sclerosis (59)). Such a scenario would help explain the detrimental impact of inhibiting UCHL1 hydrolase activity in SMA mice found in the current study. Thus, studies examining the influence of *increased* levels of UCHL1 on SMA pathology may now be warranted. However, targeting other aspects of UPS dysfunction that are directly contributing to disease pathogenesis (e.g. Uba1 suppression (26)) may prove to be more beneficial in the long run for developing novel SMA therapeutics.

In conclusion, we have demonstrated that pharmacological inhibition of UCHL1 exacerbates rather than ameliorates disease symptoms in a mouse model of SMA. As a result, pharmacological inhibition of UCHL1 is not a viable therapeutic target for the treatment of SMA. Rather, we showed that increased levels of UCHL1 in SMA represent, at least in part, a downstream consequence of decreased Uba1 levels, indicative of an attempted supportive compensatory response to defects in ubiquitin homeostasis caused by low levels of SMN protein. This provides further insights into the complex nature of perturbations in ubiquitin homeostasis driving disease pathogenesis in SMA.

This article is protected by copyright. All rights reserved.

Accepted Article

Accepted Article

## REFERENCES


1. Pearn J. Incidence, prevalence, and gene frequency studies of chronic childhood spinal muscular atrophy. Journal of medical genetics. 1978;15(6):409-13. Epub 1978/12/01.
2. Lunn MR, Wang CH. Spinal muscular atrophy. Lancet. 2008;371(9630):2120-33. Epub 2008/06/24.
3. Lefebvre S, Bürglen L, Reboullet S, Clermont O, Burlet P, Viollet L, Benichou B, Cruaud C, Millasseau P, Zeviani M, Le Paslier D, Frézal J, Cohen D, Weissenbach J, Munnich A, Melki J. Identification and characterization of a spinal muscular atrophy-determining gene. Cell. 1995;80(1):155-65.
4. Fallini C, Zhang H, Su Y, Silani V, Singer RH, Rossoll W, Bassell GJ. The survival of motor neuron (SMN) protein interacts with the mRNA-binding protein HuD and regulates localization of poly(A) mRNA in primary motor neuron axons. The Journal of neuroscience : the official journal of the Society for Neuroscience. 2011;31(10):3914-25. Epub 2011/03/11.
5. Lorson CL, Hahnen E, Androphy EJ, Wirth B. A single nucleotide in the SMN gene regulates splicing and is responsible for spinal muscular atrophy. Proceedings of the National Academy of Sciences of the United States of America. 1999;96(11):6307-11. Epub 1999/05/26.
6. Monani UR, Lorson CL, Parsons DW, Prior TW, Androphy EJ, Burghes AH, McPherson JD. A single nucleotide difference that alters splicing patterns distinguishes the SMA gene SMN1 from the copy gene SMN2. Human molecular genetics. 1999;8(7):1177-83. Epub 1999/06/17.
7. Feldkotter M, Schwarzer V, Wirth R, Wienker TF, Wirth B. Quantitative analyses of SMN1 and SMN2 based on real-time lightCycler PCR: fast and highly reliable carrier testing and prediction of severity of spinal muscular atrophy. American journal of human genetics. 2002;70(2):358-68. Epub 2002/01/16.
8. Wirth B, Brichta L, Schrank B, Lochmuller H, Blick S, Baasner A, Heller R. Mildly affected patients with spinal muscular atrophy are partially protected by an increased SMN2 copy number. Human genetics. 2006;119(4):422-8. Epub 2006/03/02.
9. Harada Y, Sutomo R, Sadewa AH, Akutsu T, Takeshima Y, Wada H, Matsuo M, Nishio H. Correlation between SMN2 copy number and clinical phenotype of spinal muscular atrophy: three SMN2 copies fail to rescue some patients from the disease severity. Journal of neurology. 2002;249(9):1211-9. Epub 2002/09/21.
10. Chung BH, Wong VC, Ip P. Spinal muscular atrophy: survival pattern and functional status. Pediatrics. 2004;114(5):e548-53. Epub 2004/10/20.
11. Lorson MA, Lorson CL. SMN-inducing compounds for the treatment of spinal muscular atrophy. Future medicinal chemistry. 2012;4(16):2067-84. Epub 2012/11/20.
12. Reyes-Turcu FE, Ventii KH, Wilkinson KD. Regulation and cellular roles of ubiquitin-specific deubiquitinating enzymes. Annual review of biochemistry. 2009;78:363-97. Epub 2009/06/06.
13. Hamilton G, Gillingwater TH. Spinal muscular atrophy: going beyond the motor neuron. Trends in molecular medicine. 2013;19(1):40-50. Epub 2012/12/12.
14. Wirth B, Garbes L, Riessland M. How genetic modifiers influence the phenotype of spinal muscular atrophy and suggest future therapeutic approaches. Current opinion in genetics & development. 2013;23(3):330-8. Epub 2013/04/23.
15. Lorson CL, Rindt H, Shababi M. Spinal muscular atrophy: mechanisms and therapeutic strategies. Human molecular genetics. 2010;19(R1):R111-8. Epub 2010/04/16.


This article is protected by copyright. All rights reserved.

16. Ciechanover A, Brundin P. The ubiquitin proteasome system in neurodegenerative diseases: sometimes the chicken, sometimes the egg. Neuron. 2003;40(2):427-46. Epub 2003/10/15.
17. Ying Z, Wang H, Wang G. The ubiquitin proteasome system as a potential target for the treatment of neurodegenerative diseases. Current pharmaceutical design. 2013;19(18):3305-14. Epub 2012/11/16.
18. Kwon DY, Dimitriadi M, Terzic B, Cable C, Hart AC, Chitnis A, Fischbeck KH, Burnett BG. The E3 ubiquitin ligase mind bomb 1 ubiquitinates and promotes the degradation of survival of motor neuron protein. Molecular biology of the cell. 2013. Epub 2013/04/26.
19. Burnett BG, Munoz E, Tandon A, Kwon DY, Sumner CJ, Fischbeck KH. Regulation of SMN protein stability. Molecular and cellular biology. 2009;29(5):1107-15. Epub 2008/12/24.
20. Hershko A, Ciechanover A. The ubiquitin system. Annual review of biochemistry. 1998;67:425-79. Epub 1998/10/06.
21. Dikic I, Robertson M. Ubiquitin ligases and beyond. BMC biology. 2012;10:22. Epub 2012/03/17.
22. D'Andrea A, Pellman D. Deubiquitinating enzymes: a new class of biological regulators. Critical reviews in biochemistry and molecular biology. 1998;33(5):337-52. Epub 1998/11/25.
23. Kwon DY, Motley WW, Fischbeck KH, Burnett BG. Increasing expression and decreasing degradation of SMN ameliorate the spinal muscular atrophy phenotype in mice. Human molecular genetics. 2011;20(18):3667-77. Epub 2011/06/23.
24. Matsumoto S, Goto S, Kusaka H, Imai T, Murakami N, Hashizume Y, Okazaki H, Hirano A. Ubiquitin-positive inclusion in anterior horn cells in subgroups of motor neuron diseases: a comparative study of adult-onset amyotrophic lateral sclerosis, juvenile amyotrophic lateral sclerosis and Werdnig-Hoffmann disease. Journal of the neurological sciences. 1993;115(2):208-13. Epub 1993/04/01.
25. Murayama S, Bouldin TW, Suzuki K. Immunocytochemical and ultrastructural studies of Werdnig-Hoffmann disease. Acta neuropathologica. 1991;81(4):408-17. Epub 1991/01/01.
26. Wishart T.M Mutsaers C.A, Riessland M, Reimer M.M, Hunter G, Hannam M.L, Eaton S, Fuller H.R, Roche S.L, Somers E, Morse R, Young P.J, Lamont D.J, Hammerschmidt M, Joshi A, Hohenstein P, Morris G.E, Parson S.H, Skehel P.A, Becker T, Robinson I.M, Becker C.G, Wirth B, Gillingwater T.H. Dysregulation of ubiquitin homeostasis and β-catenin signalling promote spinal muscular atrophy. The Journal of clinical investigation. 2014;124(4):1821-34. Epub 2014/03/03.
27. Hsu SH, Lai MC, Er TK, Yang SN, Hung CH, Tsai HH, Lin YC, Chang JG, Lo YC, Jong YJ. Ubiquitin carboxyl-terminal hydrolase L1 (UCHL1) regulates the level of SMN expression through ubiquitination in primary spinal muscular atrophy fibroblasts. Clinica chimica acta; international journal of clinical chemistry. 2010;411(23-24):1920-8. Epub 2010/08/18.
28. Day IN, Thompson RJ. UCHL1 (PGP 9.5): neuronal biomarker and ubiquitin system protein. Progress in neurobiology. 2010;90(3):327-62. Epub 2009/11/03.
29. Wilkinson KD, Lee KM, Deshpande S, Duerksen-Hughes P, Boss JM, Pohl J. The neuron-specific protein PGP 9.5 is a ubiquitin carboxyl-terminal hydrolase. Science (New York, NY). 1989;246(4930):670-3. Epub 1989/11/03.
30. Meray RK, Lansbury PT, Jr. Reversible monoubiquitination regulates the Parkinson disease-associated ubiquitin hydrolase UCH-L1. The Journal of biological chemistry. 2007;282(14):10567-75. Epub 2007/01/30.

This article is protected by copyright. All rights reserved.

31. Liu Y, Fallon L, Lashuel HA, Liu Z, Lansbury PT, Jr. The UCH-L1 gene encodes two opposing enzymatic activities that affect alpha-synuclein degradation and Parkinson's disease susceptibility. Cell. 2002;111(2):209-18. Epub 2002/11/01.
32. Osaka H, Wang YL, Takada K, Takizawa S, Setsuie R, Li H, Sato Y, Nishikawa K, Sun YJ, Sakurai M, Harada T, Hara Y, Kimura I, Chiba S, Namikawa K, Kiyama H, Noda M, Aoki S, Wada K. Ubiquitin carboxy-terminal hydrolase L1 binds to and stabilizes monoubiquitin in neuron. Human molecular genetics. 2003;12(16):1945-58. Epub 2003/08/13.
33. Xue S, Jia J. Genetic association between Ubiquitin Carboxy-terminal Hydrolase-L1 gene S18Y polymorphism and sporadic Alzheimer's disease in a Chinese Han population. Brain research. 2006;1087(1):28-32. Epub 2006/04/22.
34. Gong B, Cao Z, Zheng P, Vitolo OV, Liu S, Staniszewski A, Moolman D, Zhang H, Shelanski M, Arancio O. Ubiquitin hydrolase Uch-L1 rescues beta-amyloid-induced decreases in synaptic function and contextual memory. Cell. 2006;126(4):775-88. Epub 2006/08/23.
35. Leroy E, Boyer R, Auburger G, Leube B, Ulm G, Mezey E, Harta G, Brownstein MJ, Jonnalagada S, Chernova T, Dehejia A, Lavedan C, Gasser T, Steinbach PJ, Wilkinson KD, Polymeropoulos MH. The ubiquitin pathway in Parkinson's disease. Nature. 1998;395(6701):451-2. Epub 1998/10/17.
36. Wintermeyer P, Kruger R, Kuhn W, Muller T, Woitalla D, Berg D, Becker G, Leroy E, Polymeropoulos M, Berger K, Przuntek H, Schols L, Epplen JT, Riess O. Mutation analysis and association studies of the UCHL1 gene in German Parkinson's disease patients. Neuroreport. 2000;11(10):2079-82. Epub 2000/08/03.
37. Maraganore DM, Lesnick TG, Elbaz A, Chartier-Harlin MC, Gasser T, Kruger R, Hattori N, Mellick GD, Quattrone A, Satoh J, Toda T, Wang J, Ioannidis JP, de Andrade M, Rocca WA. UCHL1 is a Parkinson's disease susceptibility gene. Annals of neurology. 2004;55(4):512-21. Epub 2004/03/30.
38. Facheris M, Strain KJ, Lesnick TG, de Andrade M, Bower JH, Ahlskog JE, Cunningham JM, Lincoln S, Farrer MJ, Rocca WA, Maraganore DM. UCHL1 is associated with Parkinson's disease: a case-unaffected sibling and case-unrelated control study. Neuroscience letters. 2005;381(1-2):131-4. Epub 2005/05/11.
39. Snapinn KW, Larson EB, Kawakami H, Ujike H, Borenstein AR, Izumi Y, Kaji R, Maruyama H, Mata IF, Morino H, Oda M, Tsuang DW, Yearout D, Edwards KL, Zabetian CP. The UCHL1 S18Y polymorphism and Parkinson's disease in a Japanese population. Parkinsonism & related disorders. 2011;17(6):473-5. Epub 2011/02/25.
40. Bilguvar K, Tyagi NK, Ozkara C, Tuysuz B, Bakircioglu M, Choi M, Delil S, Caglayan AO, Baranoski JF, Erturk O, Yalcinkaya C, Karacorlu M, Dincer A, Johnson MH, Mane S, Chandra SS, Louvi A, Boggon TJ, Lifton RP, Horwich AL, Gunel M. Recessive loss of function of the neuronal ubiquitin hydrolase UCHL1 leads to early-onset progressive neurodegeneration. Proceedings of the National Academy of Sciences of the United States of America. 2013;110(9):3489-94. Epub 2013/01/30.
41. Hsieh-Li HM, Chang JG, Jong YJ, Wu MH, Wang NM, Tsai CH, Li H. A mouse model for spinal muscular atrophy. Nature genetics. 2000;24(1):66-70. Epub 1999/12/30.
42. Riessland M, Ackermann B, Forster A, Jakubik M, Hauke J, Garbes L, Fritzsche I, Mende Y, Blumcke I, Hahnen E, Wirth B. SAHA ameliorates the SMA phenotype in two mouse models for spinal muscular atrophy. Human molecular genetics. 2010;19(8):1492-506. Epub 2010/01/26.
43. Mutsaers CA, Lamont DJ, Hunter G, Wishart TM, Gillingwater TH. Label-free proteomics identifies Calreticulin and GRP75/Mortalin as peripherally accessible protein biomarkers for spinal muscular atrophy. Genome medicine. 2013;5(10):95. Epub 2013/10/19.

This article is protected by copyright. All rights reserved.

Accepted Article

44. Cartier AE, Ubhi K, Spencer B, Vazquez-Roque RA, Kosberg KA, Fourgeaud L, Kanayson P, Patrick C, Rockenstein E, Patrick GN, Masliah E. Differential effects of UCHL1 modulation on alpha-synuclein in PD-like models of alpha-synucleinopathy. PloS one. 2012;7(4):e34713. Epub 2012/04/20.
45. Murray LM, Comley LH, Thomson D, Parkinson N, Talbot K, Gillingwater TH. Selective vulnerability of motor neurons and dissociation of pre- and post-synaptic pathology at the neuromuscular junction in mouse models of spinal muscular atrophy. Human molecular genetics. 2008;17(7):949-62. Epub 2007/12/11.
46. Passini MA, Bu J, Roskelley EM, Richards AM, Sardi SP, O'Riordan CR, Klinger KW, Shihabuddin LS, Cheng SH. CNS-targeted gene therapy improves survival and motor function in a mouse model of spinal muscular atrophy. The Journal of clinical investigation. 2010;120(4):1253-64. Epub 2010/03/18.
47. Eaton SL, Roche SL, Llavero Hurtado M, Oldknow KJ, Farquharson C, Gillingwater TH, Wishart TM. Total protein analysis as a reliable loading control for quantitative fluorescent Western blotting. PloS one. 2013;8(8):e72457. Epub 2013/09/12.
48. Cartier AE, Djakovic SN, Salehi A, Wilson SM, Masliah E, Patrick GN. Regulation of synaptic structure by ubiquitin C-terminal hydrolase L1. The Journal of neuroscience : the official journal of the Society for Neuroscience. 2009;29(24):7857-68. Epub 2009/06/19.
49. Satheshkumar PS, Anton LC, Sanz P, Moss B. Inhibition of the ubiquitin-proteasome system prevents vaccinia virus DNA replication and expression of intermediate and late genes. Journal of virology. 2009;83(6):2469-79. Epub 2009/01/09.
50. Rinetti GV, Schweizer FE. Ubiquitination acutely regulates presynaptic neurotransmitter release in mammalian neurons. The Journal of neuroscience : the official journal of the Society for Neuroscience. 2010;30(9):3157-66. Epub 2010/03/06.
51. Mayer RJ. From neurodegeneration to neurohomeostasis: the role of ubiquitin. Drug news & perspectives. 2003;16(2):103-8. Epub 2003/06/07.
52. Chen PC, Bhattacharyya BJ, Hanna J, Minkel H, Wilson JA, Finley D, Miller RJ, Wilson SM. Ubiquitin homeostasis is critical for synaptic development and function. The Journal of neuroscience : the official journal of the Society for Neuroscience. 2011;31(48):17505-13. Epub 2011/12/02.
53. Setsuie R, Wang YL, Mochizuki H, Osaka H, Hayakawa H, Ichihara N, Li H, Furuta A, Sano Y, Sun YJ, Kwon J, Kabuta T, Yoshimi K, Aoki S, Mizuno Y, Noda M, Wada K. Dopaminergic neuronal loss in transgenic mice expressing the Parkinson's disease-associated UCH-L1 I93M mutant. Neurochemistry international. 2007;50(1):119-29. Epub 2006/09/13.
54. Elbaz A, Levecque C, Clavel J, Vidal JS, Richard F, Correze JR, Delemotte B, Amouyel P, Alperovitch A, Chartier-Harlin MC, Tzourio C. S18Y polymorphism in the UCH-L1 gene and Parkinson's disease: evidence for an age-dependent relationship. Movement disorders : official journal of the Movement Disorder Society. 2003;18(2):130-7. Epub 2003/01/23.
55. Choi J, Levey AI, Weintraub ST, Rees HD, Gearing M, Chin LS, Li L. Oxidative modifications and down-regulation of ubiquitin carboxyl-terminal hydrolase L1 associated with idiopathic Parkinson's and Alzheimer's diseases. The Journal of biological chemistry. 2004;279(13):13256-64. Epub 2004/01/15.
56. Chen F, Sugiura Y, Myers KG, Liu Y, Lin W. Ubiquitin carboxyl-terminal hydrolase L1 is required for maintaining the structure and function of the neuromuscular junction. Proceedings of the National Academy of Sciences of the United States of America. 2010;107(4):1636-41. Epub 2010/01/19.
57. Saigoh K, Wang YL, Suh JG, Yamanishi T, Sakai Y, Kiyosawa H, Harada T, Ichihara N, Wakana S, Kikuchi T, Wada K. Intragenic deletion in the gene encoding ubiquitin

This article is protected by copyright. All rights reserved.

Accepted Article

carboxy-terminal hydrolase in gad mice. Nature genetics. 1999;23(1):47-51. Epub 1999/09/02.
58. Kwon J, Wada K. The Gad Mouse: A Window Into UPS-Related Neurodegeneration and the Function of the Function of the Deubiquitinating Enzyme Uch-L1. In: Stefanis L, Keller J, editors. The Proteasome in Neurodegeneration: Springer US; 2006. p. 185-98.
59. Yasvoina MV, Genc B, Jara JH, Sheets PL, Quinlan KA, Milosevic A, Shepherd GM, Heckman CJ, Ozdinler PH. eGFP Expression under UCHL1 Promoter Genetically Labels Corticospinal Motor Neurons and a Subpopulation of Degeneration-Resistant Spinal Motor Neurons in an ALS Mouse Model. The Journal of neuroscience : the official journal of the Society for Neuroscience. 2013;33(18):7890-904. Epub 2013/05/03.

## AUTHOR CONTRIBUTIONS

RAP, TMW & THG conceived, designed and coordinated the project; RAP, CAM, TMW, GH & THG designed and performed experiments; RAP, CAM & THG analyzed data; BW contributed reagents; all authors contributed to writing the paper.

## ACKNOWLEDGEMENTS

This work was supported by grants from the Muscular Dystrophy Campaign (THG & GH), the Anatomical Society (THG & RAP), the SMA Trust (THG), the Deutsche Forschungsgemeinschaft, EU FP7/2007-2013 grant No 2012-305121 (NeurOmics; BW) and Center for Molecular Medicine Cologne (BW). TMW is currently a Career Track Fellow at the Roslin Institute, supported by BBSRC ISPG funding.

## CONFLICT OF INTEREST STATEMENT

The authors do not have any conflicting interests to declare.

Accepted Article

This article is protected by copyright. All rights reserved.

Accepted Article

## FIGURE LEGENDS

**Figure 1. Increased UCHL1 levels in Type I SMA patient primary fibroblasts. A.** Top panel shows representative fluorescent western blot bands for UCHL1 protein from primary fibroblasts from three individual Type I SMA patients and unaffected controls. Order of lanes: Control ML 32, SMA ML 83, Control ML 44, SMA ML17, Control ML 24, SMA ML 16. Ponceau S loading control is shown in the bottom panel. **B.** Bar chart showing quantification of UCHL1 fluorescent western blot band intensity in SMA and control human fibroblast samples, normalized to Ponceau S (N=3 fibroblast samples per genotype; $^{**}P < 0.01$; two-tailed unpaired Student's t-test).

**Figure 2. Increased UCHL1 levels in 'Taiwanese' SMA mouse spinal cord and skeletal muscle. A & D.** Middle panel shows representative fluorescent western blot bands for UCHL1 protein in whole (**A**) spinal cord and (**D**) muscle protein extract from P10 SMA and control mice. Ponceau S loading control is shown in the bottom panel. The genotype of the corresponding mice, as analysed by PCR, is shown in the top panel. **B & E.** Bar chart showing quantification of UCHL1 fluorescent western blot band intensity in SMA and control mice, normalised to Ponceau S, in spinal cord (**B**) (N=4 mice per genotype; $^{***}P < 0.005$; two-tailed unpaired Student's t-test) and muscle (**E**) (N=3 mice per genotype; $^{**}P < 0.01$; two-tailed unpaired Student's t-test). **C & F.** Immunohistochemical staining of UCHL1 in the (**C**) ventral horn of the spinal cord and (**F**) *gastrocnemius* muscle of P10 control and SMA mice. Micrographs were obtained from tissue processed in an identical manner and with identical microscope settings for control and SMA tissue. Scale bars represent 200µm for spinal cord and 100µm for muscle images. **G.** Graph showing UCHL1 levels in the *gastrocnemius* muscle of control and SMA mice at P1, P4, P7 and P9 measured using quantitative fluorescent western blot (N=3 mice per genotype; $^{**}P < 0.01$, $^{*}P < 0.05$, ns = not significant; two-tailed unpaired Student's t-test).

**Figure 3. Pharmacological inhibition of UCHL1 reduces mono-ubiquitin levels but has no effect on SMN levels in SMA mouse spinal cord *in vivo*. A & C.** Representative fluorescent western blots showing (**A**) mono-ubiquitin levels and (**C**) SMN levels from whole spinal cord protein extract from vehicle and LDN-57444 treated P10 SMA mice. Ponceau S loading control is shown in the bottom panels. Mice were administered with 0.5 mg/kg LDN-57444 dissolved in DMSO twice daily via intraperitoneal injection from the day of birth. The same volume of DMSO alone was used as a vehicle-only control. **B & D.** Bar chart showing quantification of (**B**) mono-ubiquitin levels and (**D**) SMN levels in vehicle and LDN-57444 treated mice (N=3 mice per treatment group; $^{*}P < 0.05$, ns = not significant; two-tailed unpaired Student's t-test).

**Figure 4. Pharmacological inhibition of UCHL1 failed to improve weight or survival of SMA mice, and precipitated the onset of weight loss. A.** Graph showing average weights

This article is protected by copyright. All rights reserved.

of vehicle and LDN-57444 treated SMA mice, as well as vehicle and LDN-57444 treated littermate control mice, from the day of birth. Mice were administered with 0.5 mg/kg LDN-57444 dissolved in DMSO or DMSO vehicle control twice daily via intraperitoneal injection from P1. **B.** Survival curves showing percentage survival of vehicle and LDN-57444 treated SMA mice, as well as vehicle and LDN-57444 treated littermate control mice. Survival curves for vehicle treated SMA mice and LDN-57444 treated SMA mice showed no significant difference when compared using a log-rank (Mantel-Cox) test. Median age of death of vehicle treated SMA mice was P11 (N=11) compared to P10 for LND-57444 treated SMA mice (N=10). **C.** Bar chart comparing age of onset of weight loss in vehicle treated SMA mice with LDN-57444 treated SMA mice. Data shown as mean ± SEM. The mean age of onset of weight loss was significantly reduced in LDN-57444 treated SMA mice compared to vehicle treated mice (N=11 vehicle treated mice, N=10 LDN-57444 treated mice; * $P < 0.05$; two-tailed unpaired Student's t-test).

**Figure 5. Pharmacological inhibition of UCHL1 had no effect on motor performance of SMA mice. A-C.** Bar charts showing the time taken for littermate control vehicle treated mice, littermate control LDN-57444 treated mice, SMA vehicle treated mice and SMA LDN-57444 treated mice to right themselves onto their paws once placed on their back at (**A**) P3, (**B**) P6 and (**C)** P9. Data are shown as mean ± SEM. Mice were administered with 0.5 mg/kg LDN-57444 dissolved in DMSO or DMSO only control twice daily via intraperitoneal injection from the day of birth (P3: control vehicle treated mice, N=19; control LDN-57444, N=15; SMA vehicle, N=17; SMA LDN-57444, N=10) (P6 control vehicle, N=16; control LDN-57444, N=12; SMA vehicle, N=15; SMA LDN-57444, N=9) (P9: control vehicle, N=16; control LDN-57444, N=12; SMA vehicle, N=11; SMA LDN-57444, N=6). Statistical comparisons were made using ANOVA with Turkey's *post hoc* comparisons test (ns = not significant). **D-F.** Representative photographs of control vehicle, SMA vehicle and SMA LDN-57444 treated mice at (**D**) P3, (**E**) P6 and (**F**) P9.

**Figure 6. Pharmacological inhibition of UCHL1 had no effect on neuromuscular pathology in SMA mice. A.** Representative micrographs of motor neuron cell soma in the ventral grey horn of spinal cord from littermate control and SMA mice at P8 treated with LDN-57444 or vehicle control. **B.** Bar chart comparing number of motor neuron soma in SMA and littermate control mice treated with LDN-57444 or vehicle control. As expected, the mean number of motor neurons was significantly reduced in vehicle treated SMA mice compared to vehicle treated littermate controls (N=4 mice per treatment/genotype; ** $P < 0.01$; ANOVA with Turkey's *post hoc* test). There was no significant difference between LDN-57444 treated and vehicle treated SMA mice (ns $P > 0.05$). **C.** Representative phase contrast micrographs of single teased muscle fibres from the TVA muscle of littermate control and SMA mice at P8 treated with LDN-57444 or vehicle control. **D-E.** Bar charts comparing muscle fibre diameters in the TVA (D) and LAL (E) muscle from SMA and littermate control mice treated with LDN-57444 or vehicle control. As expected, the mean muscle fibre diameter was significantly reduced in vehicle treated SMA mice compared to vehicle treated littermate controls for both muscles (N=3 mice per treatment/genotype; ** $P < 0.01$; *** $P < 0.001$; ANOVA with Turkey's *post hoc* test). There was no significant

This article is protected by copyright. All rights reserved.

Accepted Article

difference between LDN-57444 treated and vehicle treated SMA mice in either muscle examined (ns $P > 0.05$). **F.** Representative confocal micrographs of immunohistochemically labelled neuromuscular junctions (NMJs) from the caudal band of the LAL muscle of littermate control and SMA mice at P8 treated with LDN-57444 or vehicle control (green = axons and synaptic terminals; red = postsynaptic acetylcholine receptors). **G.** Bar chart comparing the average number of motor axon inputs per NMJ in SMA and littermate control mice treated with LDN-57444 or vehicle control. As expected, the mean number of axon inputs was significantly reduced in vehicle treated SMA mice compared to vehicle treated littermate controls (N=4 mice per treatment/genotype; * $P < 0.05$; ANOVA with Turkey's *post hoc* test). There was no significant difference between LDN-57444 treated and vehicle treated SMA mice (ns $P > 0.05$). Scale bars represent 200µm for spinal cord images, 25µm for muscle images and 50µm for NMJ images. Data shown as mean ± SEM.

**Figure 7. Inhibition of Uba1 is sufficient to increase UCHL1 levels in neurons. A.** Representative fluorescent western blot of protein levels in primary neurons treated with 50uM UBEI-41 (a cell-permeable ubiquitin E1 inhibitor), or DMSO only vehicle control, for 2 hours. The top panel shows mono-ubiquitin protein levels, the middle panel shows UCHL1 protein levels and the bottom panel shows beta-actin loading control levels. (**B**) Bar chart showing levels of mono-ubiquitin protein in control and UBEI-41 treated cells (N=4 independent experiments per treatment; ** $P < 0.01$; two-tailed unpaired Student's t-test). (**C**) Bar chart showing levels of UCHL1 in control and UBEI-41 treated cells (N=4 independent experiments per treatment, **** $P < 0.001$; two-tailed unpaired Student's t-test). Data shown as mean ± SEM.

**Supplementary Figure 1. Secondary antibody only immunohistochemistry control. A-D.** Secondary antibody only immunohistochemical staining of the ventral horn of the spinal cord of P10 control mouse (**A**) spinal cord, (**C**) muscle and SMA mouse (**B**) spinal cord, (**D**) muscle without inclusion of UCHL1 primary antibody. Micrographs were obtained from tissue processed in an identical manner and with identical microscope settings. Scale bars represent 200µm for spinal cord and 100µm for muscle.

This article is protected by copyright. All rights reserved.

Accepted Article

Accepted Article

Neuropathology and Applied Neurobiology

## CONFLICT OF INTEREST

**Title: Pharmacological inhibition of UCHL1 is not a valid therapeutic approach for the treatment of spinal muscular atrophy**

**Name: Powis et al. (Corresponding author: Professor T Gillingwater)**

As the corresponding author of the above manuscript which has been submitted to *Neuropathology and Applied Neurobiology*, please list below all co-authors stating whether or not they have any possible conflicts of interest. Only conflicts of interest specific to this manuscript need be declared. Please return the completed form by email or fax to the editorial office.

The following are examples of possible conflicts of interest:

1. Source of funding
2. Paid consult to sponsor
3. Study investigator funded by sponsor
4. Employee of sponsor
5. Board membership with sponsor
6. Stock holder for mentioned product
7. Patent inventor for mentioned product
8. Any financial relationship to competitors of mentioned product

This information will be kept confidential. The Editor will discuss the method of disclosure of any potential conflict of interest with authors on an individual basis.

| *Author* | *No Conflict* | *Conflict (Please specify)* |
|---|---|---|
| *R Powis* | *X* | |
| *C Mutsaers* | *X* | |
| *T Wishart* | *X* | |
| *G Hunter* | *X* | |
| *B Wirth* | *X* | |
| *T Gillingwater* | *X* | |

**Multiple Authorship**

Please tick the box to confirm the following statement:

*The corresponding author states that all authors have seen and approved the manuscript.* X

This article is protected by copyright. All rights reserved.

Accepted Article

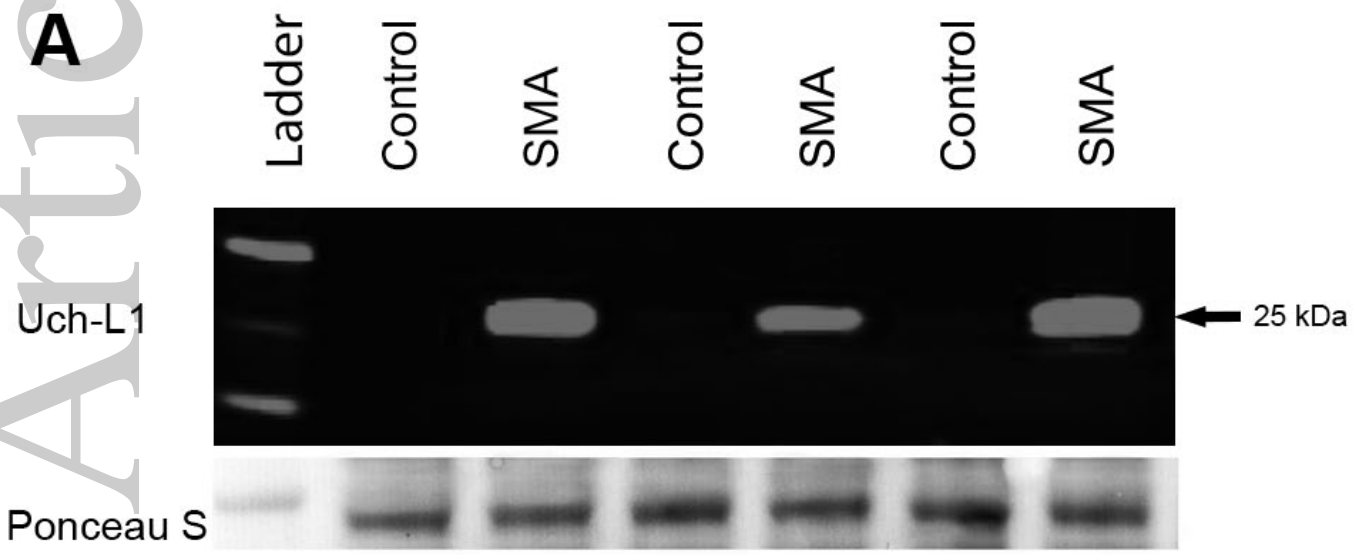


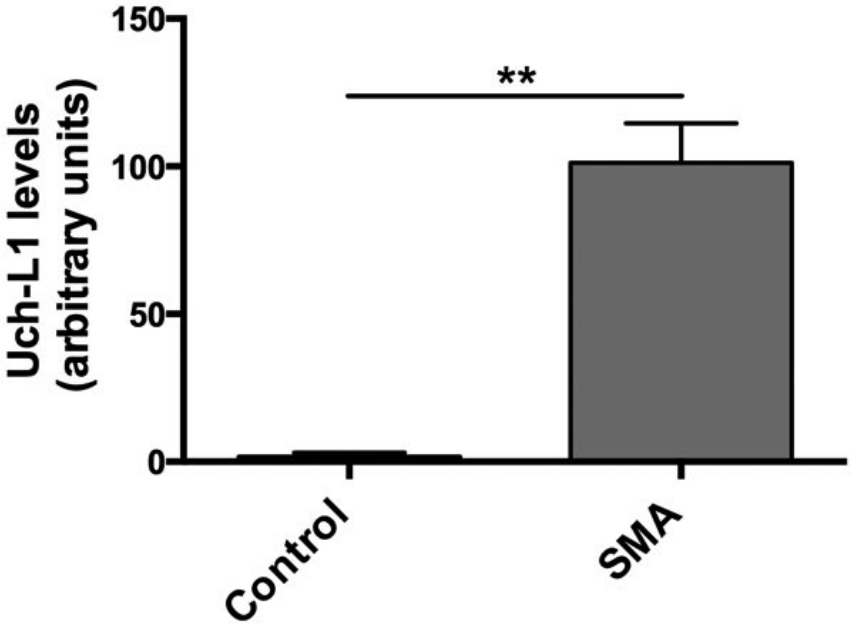


nan_12168_fig1.tiff

Accepted Article

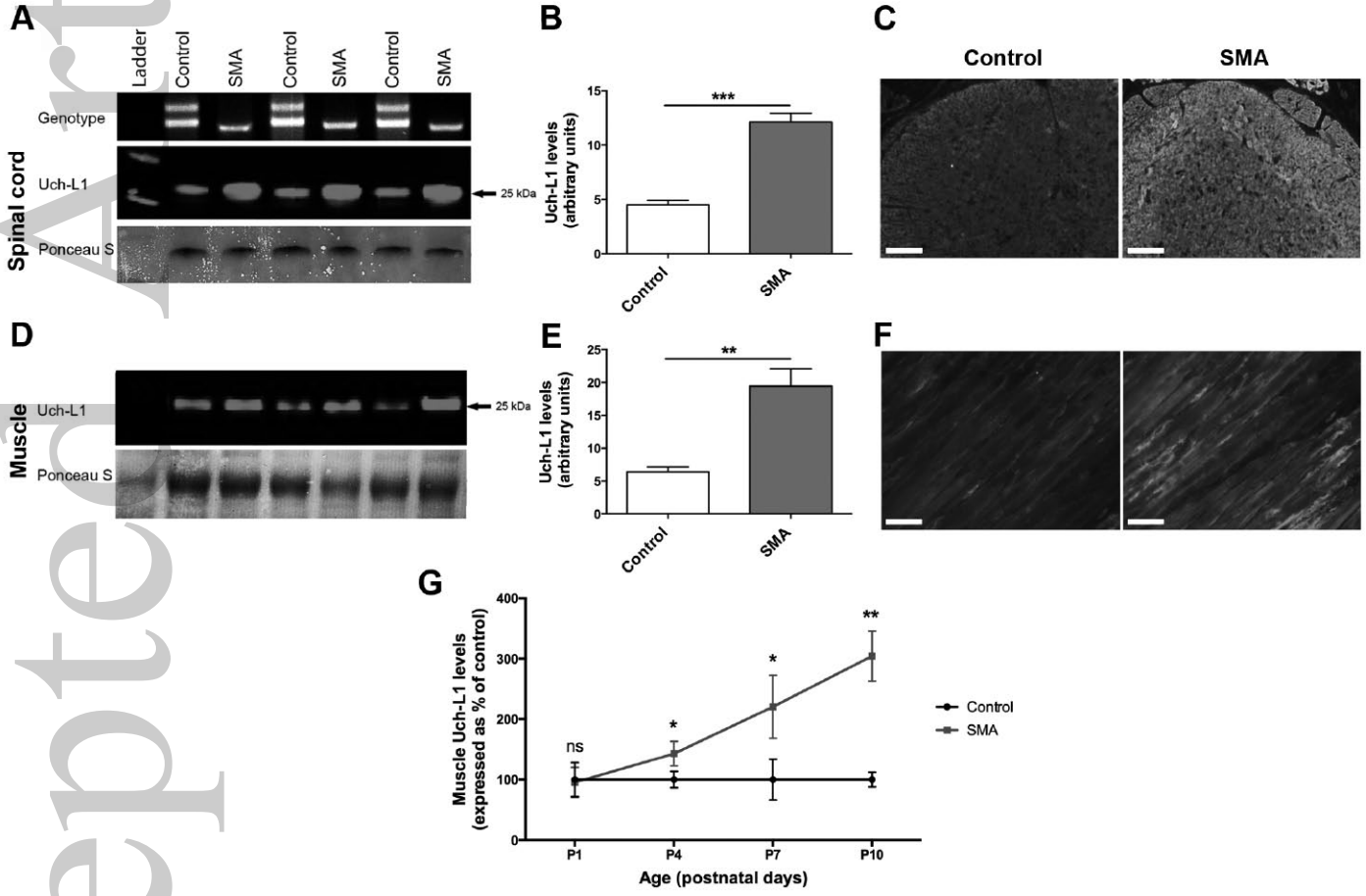


nan_12168_fig2.tiff

Accepted Article

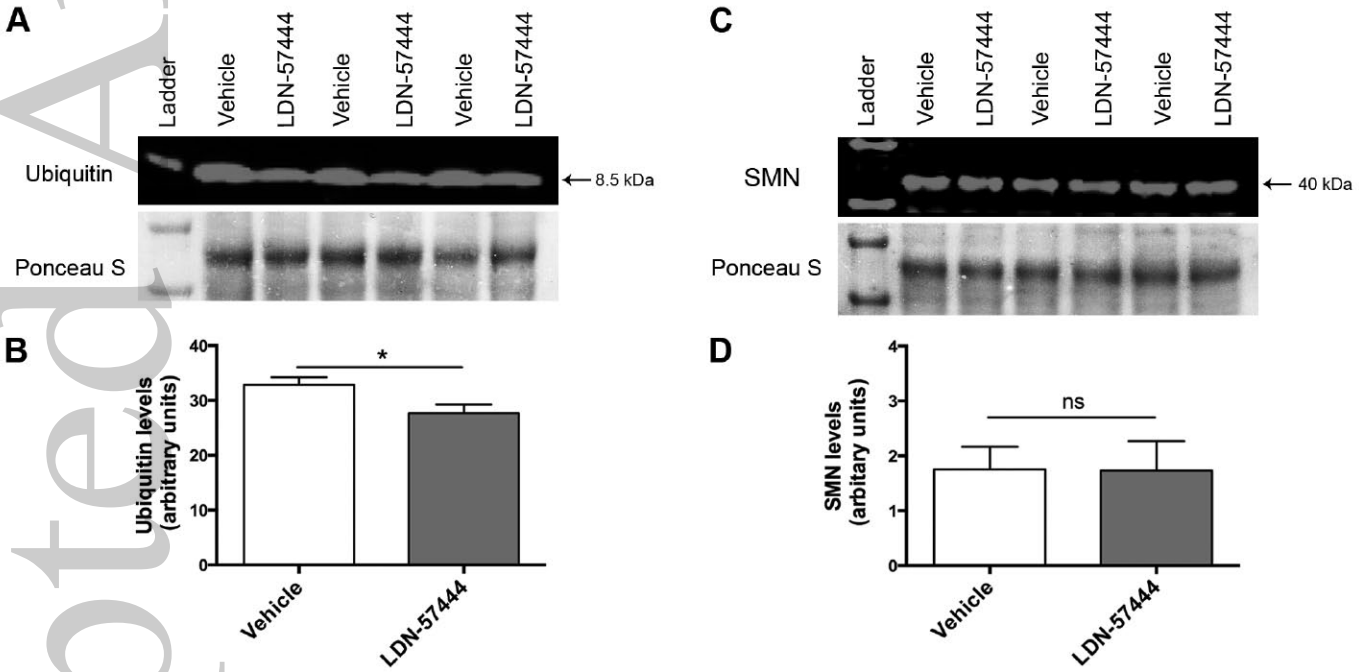


nan_12168_fig3.tiff

Accepted Article

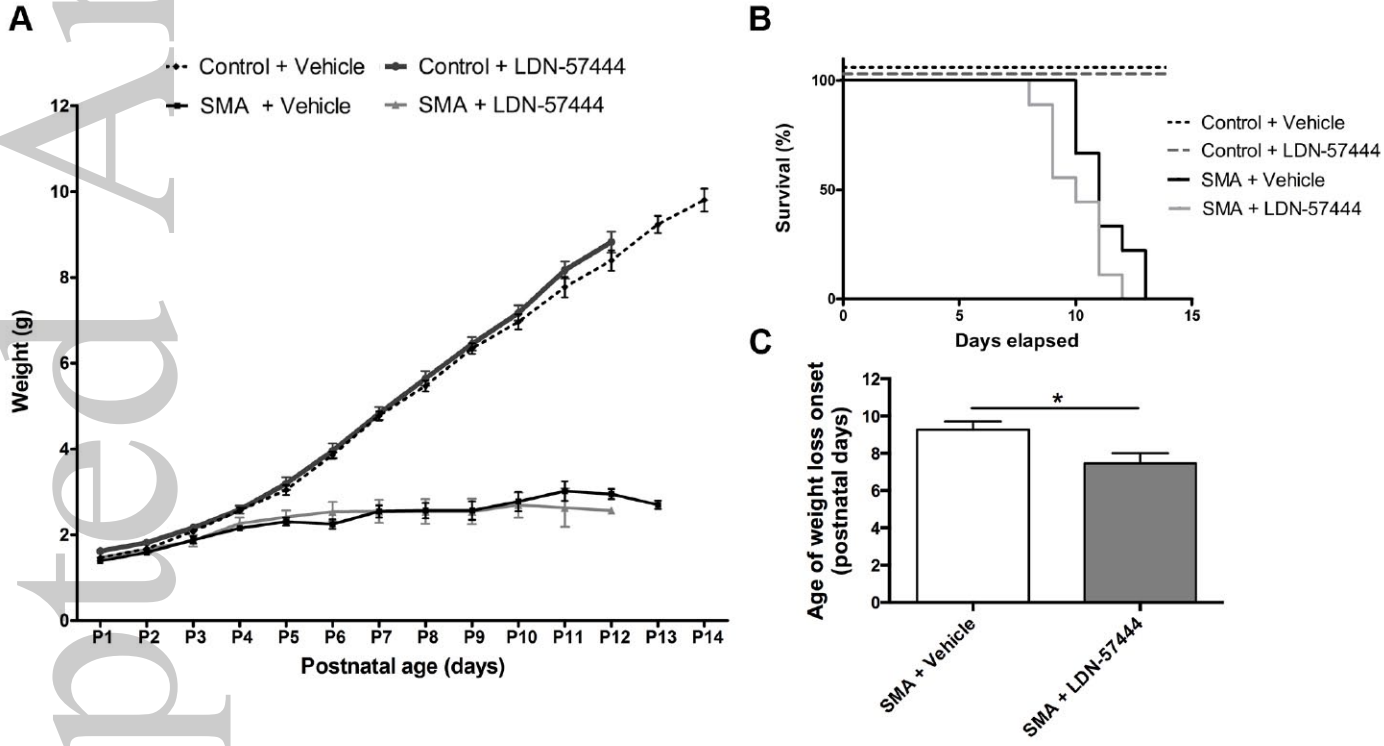


nan_12168_fig4.tiff

Accepted Article

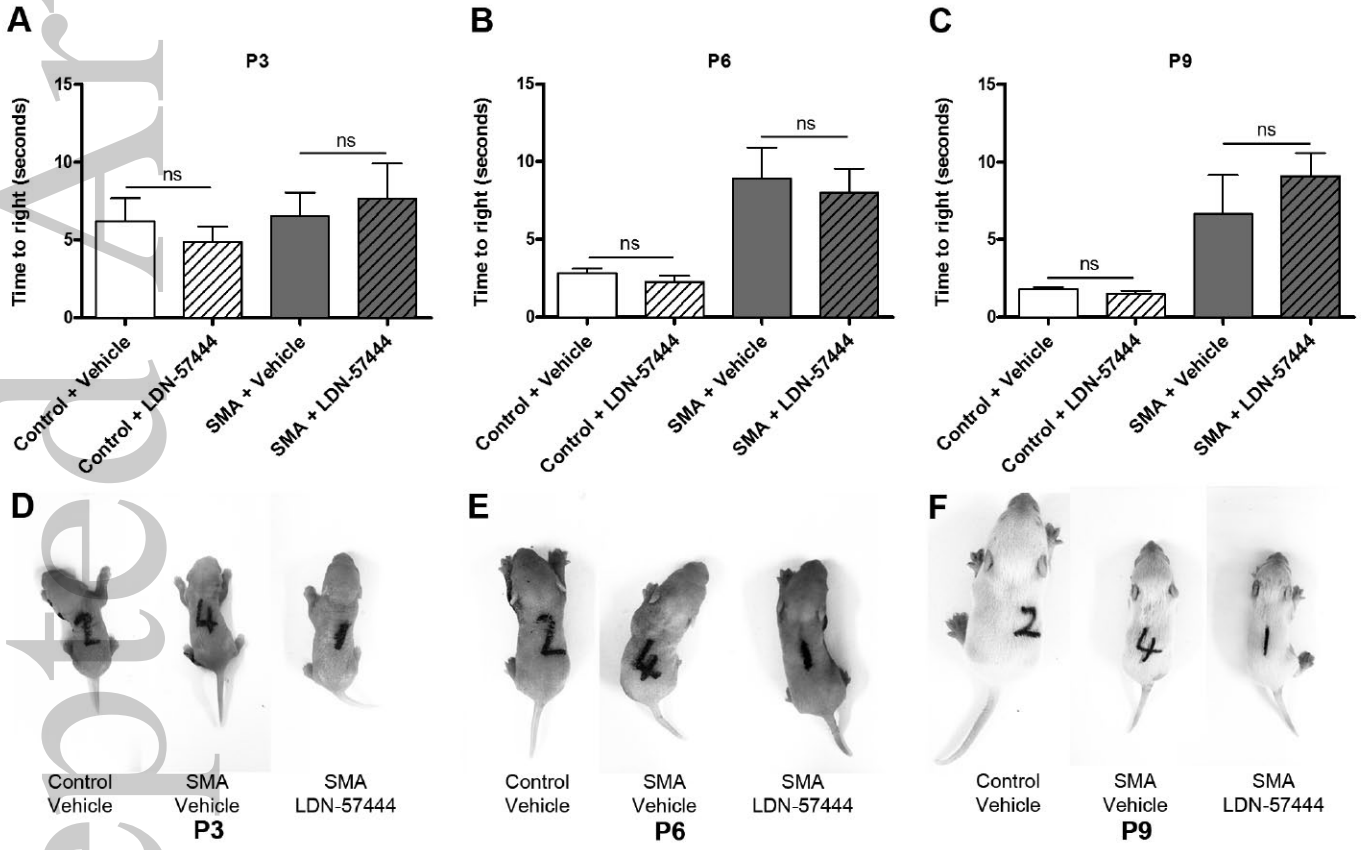


nan_12168_fig5.tiff

Accepted Article

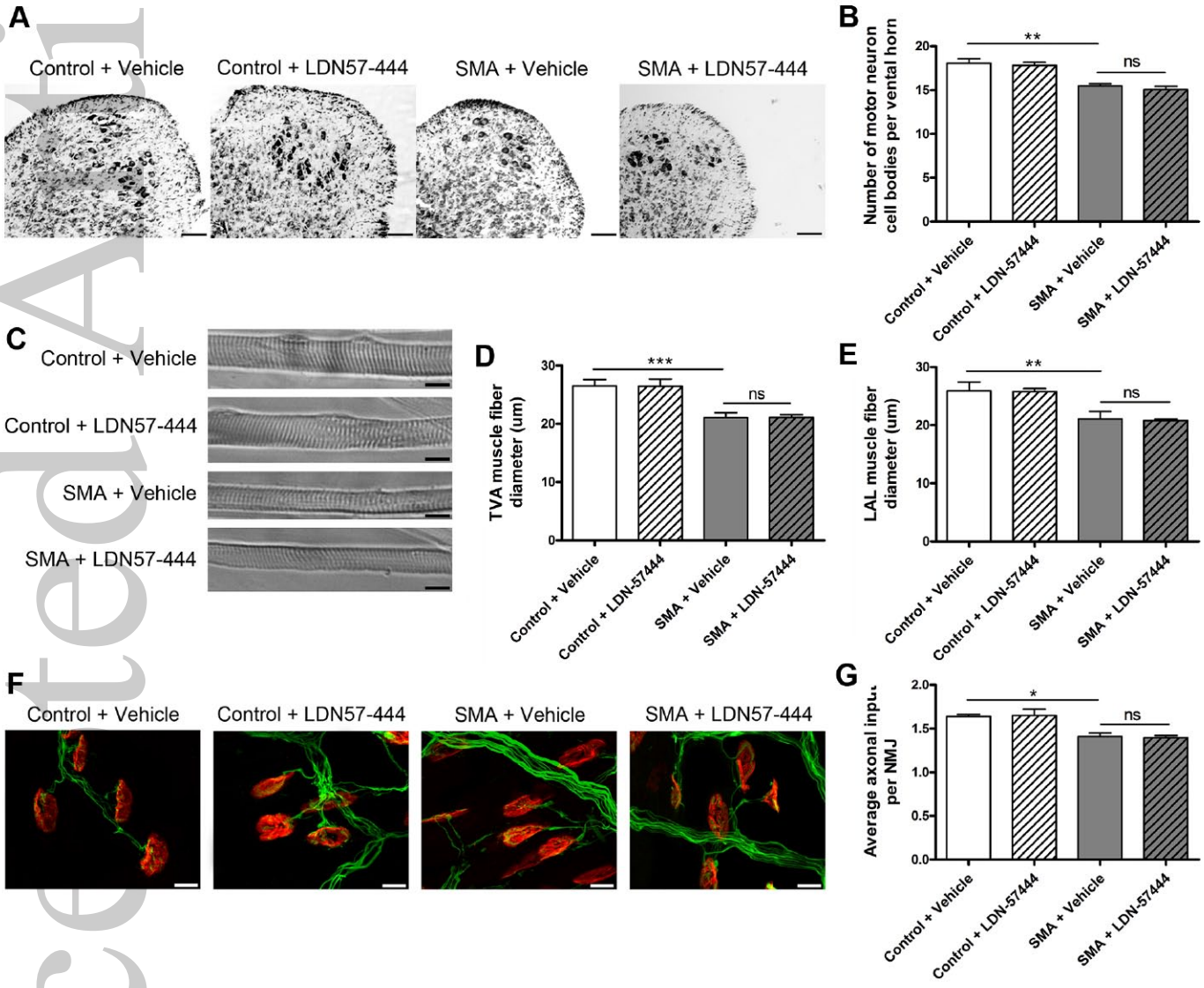


nan_12168_fig6.tiff

Accepted Article

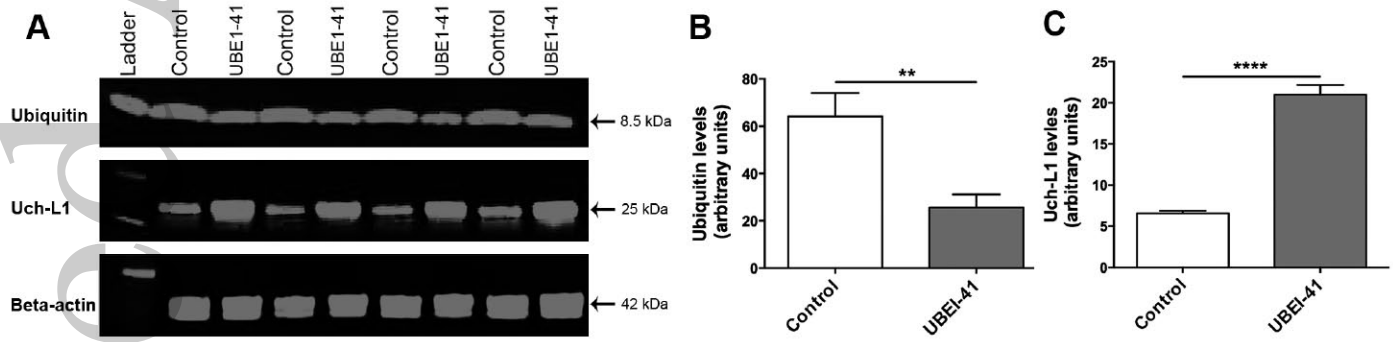


nan_12168_fig7.tiff